JOURNAL OF GEOPHYSICAL RESEARCH, VOL. 103, NO. D7, PAGES 8455–8464, APRIL 20, 1998

A critical analysis of the Stratospheric Aerosol and Gas Experiment II spectral inversion algorithm

Didier Fussen

Belgian Institute for Space Aeronomy, Brussels, Belgium

Abstract. The ozone long-term trends derived from the Stratospheric Aerosol and Gas Experiment II have been shown to be biased by the level of volcanic aerosol. We have investigated the spectral algorithm used to separate the partial optical thicknesses associated with ozone and aerosols. We present two possible causes of inaccuracies capable of producing relative errors on the slant path ozone optical thickness as large as 5–15%. The first one is related to the interpolation of the aerosol optical thickness at 0.6 μm which is not very well performed by solving the inverse problem of the unknown size distribution. The second error cause lies in the assumed altitude independence of the aerosol optical properties. Both error causes are discussed, and possible corrections are presented.

1. Introduction

Since its launch in October 1984, the Stratospheric Aerosol and Gas Experiment (SAGE II) has provided important information on long-term changes in stratospheric ozone, nitrogen dioxide, water vapor, and aerosol concentration profiles. The instrument is a seven-channel Sun photometer making measurements of the Earth's limb transmittance during orbital sunrises and sunsets. The nominal wavelengths are 0.385, 0.448, 0.453, 0.525, 0.600, 0.940, and 1.02 μm, and a 1-km vertical resolution is achieved [*Mauldin et al.*, 1985].

The inversion algorithm has been discussed by *Chu et al.* [1989], and the retrieved concentration profiles for O_3, NO_2, and aerosols can be obtained on request from the NASA Earth Observing System Data and Information System, Langley Research Center. There exists a large number of publications concerning the validation of the SAGE II experiment, and the interested reader should refer to the special issue of *Journal of Geophysical Research* (*94*(D6), 8335–8466, 1989) and all references therein.

Very recently, however, systematic comparisons [*Wang et al.*, 1996] between the ozone profiles retrieved by SAGE II and by the solar backscattered ultraviolet (SBUV) instrument [*Hood et al.*, 1993] have shown that the SAGE II ozone values must be corrected for aerosol interference. The spurious coupling between ozone and aerosol retrievals had already been suspected [*Cunnold and Veiga*, 1991] and became clearly evident in coincident measurements over the post-Pinatubo period September 1991 to December 1993 [*Cunnold et al.*, 1996]. At altitudes below 30 km the SAGE II ozone retrievals were found to be biased by the large aerosol concentrations. The bias is a nonlinear function of the aerosol extinction coefficient for lower altitudes. An important consequence is the probable overestimation of the decreasing trend of the total stratospheric ozone column in the tropics by about 0.2% per year, which accounts for approximately one half of the difference between SAGE II and total ozone mapping spectrometer (TOMS) ozone trends.

The above mentioned authors attribute the aerosol interference effect to the interpolation of the SAGE II aerosol extinction at 0.6 μm and also to the evolution of the aerosol size distribution during the volcanic aerosol relaxation. Empirical estimations of the aerosol extinction deficit at 0.6 μm as large as 8% have been reported. However, neither *Cunnold et al.* [1996] nor *Wang et al.* [1996] provided a real explanation of the error or a possible correcting algorithm. The purpose of the present work is to discuss two possible causes of the problem in the frame of a simplified description of the spectral inversion problem.

Paper number 97JD03737.
0148-0227/98/97JD-03737$09.00

2. SAGE II Spectral Inversion Algorithm

We recall here briefly the main steps leading to the derivation of the ozone and aerosol slant path optical thicknesses as described by *Chu et al.* [1989]. After having subtracted the Rayleigh scattering and the estimated NO_2 contributions, the slant path total optical thickness δ_λ at wavelength λ is given by

$$\delta_\lambda(h) = \int \beta_\lambda(z(l(h)))\, dl \tag{1}$$

where the integral runs over the optical path l and $\beta_\lambda(z)$ is the altitude-dependent total extinction coefficient, both quantities depending on the ray tangent height h. The aerosol (x_i), ozone $(a_i y)$ and total (δ_i) $(i = 1, 3, 4, 5, 7)$ slant path optical thicknesses at $\lambda_1 = 1.02$ μm, $\lambda_3 = 0.6$ μm, $\lambda_4 = 0.525$ μm, $\lambda_5 = 0.453$ μm, and $\lambda_7 = 0.385$ μm are related by the following system of five equations and six unknowns (for the sake of coherence we have used the same indices as *Chu et al.* [1989]):

$$x_1 = \delta_1 \tag{2}$$

$$x_3 + a_3 y = \delta_3 \tag{3}$$

$$x_4 + a_4 y = \delta_4 \tag{4}$$

$$x_5 + a_5 y = \delta_5 \tag{5}$$

$$x_7 = \delta_7 \tag{6}$$

where

$$a_i y = \delta_i^{O_3} \; (a_1 \simeq 0,\; a_3 = 1,\; a_4 = 0.439,$$

$$a_5 = 0.0338,\; a_7 \simeq 0) \tag{7}$$

The values of the a_i coefficients are determined by the ratios of the respective cross sections $\sigma_i^{O_3}$ (assumed to be altitude independent), while the maximum of the Chappuis band at $\lambda_3 = 0.6$ μm is arbitrarily chosen as a reference to define y. If n_{O_3} is the ozone number density, we have

$$a_3 y = y = \int \sigma_3^{O_3} n_{O_3}(l)\, dl = \sigma_3^{O_3} N_{O_3}$$

$$= \frac{\sigma_3^{O_3}}{\sigma_i^{O_3}} \delta_i^{O_3} \; (i = 4, 5, 7) \tag{8}$$

where $N_{O_3} = \int n_{O_3}(l)\, dl$. The situation is more complicated for the aerosol optical thickness because the aerosol total extinction coefficient results from the integration of an unknown particle size distribution multiplied by the corresponding attenuation cross section, which is, of course, size-dependent. Assuming spherical particles of radius r, one may write

$$\beta_\lambda^{\text{aerosol}} = \int_0^\infty Q(\lambda, r) \frac{dn^{\text{aerosol}}}{dr} dr \simeq \int_0^R Q(\lambda, r) \frac{dn^{\text{aerosol}}}{dr} dr \tag{9}$$

where dn^{aerosol}/dr stands for the size distribution function. It is generally accepted that the standard stratospheric aerosol could consist of homogeneous particles ($\frac{3}{4}$ H_2SO_4 + $\frac{1}{4}$ H_2O, by weight) and that the attenuation cross section Q may be reasonably described in the frame of the Mie theory. The most difficult parameters to estimate are obviously those associated with the size distribution function due to the small number of spectral channels considered. As a consequence, the relationship between x_3 and $\{x_1, x_4, x_5, x_7\}$ is not known, or, equivalently, the spectral variation of the aerosol optical thickness as a function of wavelength is a product of the retrieval process, not an input data.

In the generic SAGE II algorithm, equation (9) was discretized over a large number of mean radii r_j, $\{j = 1, 2, \ldots m\}$, up to the largest significative radius $R \equiv r_m$, and integrated along the optical path, leading to the linear underdetermined system

$$\vec{x} = Q\vec{N} \tag{10}$$

or

$$\begin{pmatrix} x_1 \\ x_4 \\ x_5 \\ x_7 \end{pmatrix} = \begin{pmatrix} Q_{11} & Q_{12} & \cdots & \cdots & Q_{1m} \\ Q_{41} & Q_{42} & \cdots & \cdots & Q_{4m} \\ Q_{51} & Q_{52} & \cdots & \cdots & Q_{5m} \\ Q_{71} & Q_{72} & \cdots & \cdots & Q_{7m} \end{pmatrix} \begin{pmatrix} N_1 \\ N_2 \\ \cdots \\ \cdots \\ N_m \end{pmatrix} \tag{11}$$

where the N_j are the slant path integrated aerosol number densities associated with the radii r_j and $Q_{ij} = Q(\lambda_i, r_j)\, \Delta r_j$.

In order to coherently retrieve six unknowns (y, x_1, x_3, x_4, x_5, x_7) from (2)–(6), a supplementary equation had to be formulated. *Chu et al.* [1989] have inverted (10) by using the Twomey's linear constraint method [*Twomey*, 1985]:

$$\vec{N} = Q^T(QQ^T + \Gamma)^{-1}\vec{x} \tag{12}$$

This solution takes the estimated noise level Γ in all channels into account and can generate the subsidiary equation by correlating the aerosol optical thickness (x_3) at 0.6 μm with the aerosol optical thicknesses at other wavelengths:

$$x_3 = \sum_{j=1}^{m} Q_{3j} N_j \tag{13}$$

or

$$x_3 = \alpha_1 x_1 + \alpha_4 x_4 + \alpha_5 x_5 + \alpha_7 x_7 \tag{14}$$

where the coefficients α_i are obtained by combining (12) and (13) as:

$$\vec{\alpha}^T = \vec{Q}_3^T \cdot Q^T(QQ^T + \Gamma)^{-1} \tag{15}$$

$$\vec{Q}_3^T = (Q_{31} Q_{32} \cdots Q_{3m}) \tag{16}$$

It is clear that the accuracy of the prediction of x_3 has a direct influence on the ozone optical thickness derivation via (3), and *Chu et al.* [1989, p. 8342] commented upon their method as follows: "... due to the very limited number of channels, the method would necessarily produce solutions that are compatible with the aerosol size distribution being very smooth and unstructured."

3. A Simple Model for the Aerosol Optical Thickness

We have used a simplified model to estimate the aerosol optical thickness and to analyze the validity of the above mentioned algorithm. Nevertheless, the model captures all the main characteristics of the light attenuation by the aerosols and is very easy to implement.

In our model we describe the aerosol size distribution function as a function of two variables:

$$\frac{dn^{\text{aerosol}}}{dr} \equiv F(r, z) \equiv n(z) f(r)$$

$$= n_0 \exp\left(-\left(\frac{z - z_0}{\Delta} \right)^2 \right) \frac{1}{r\sqrt{2\pi}\ln(s)} \exp\left(-\frac{\ln^2\left(\frac{r}{r_0}\right)}{2\ln^2(s)} \right) \tag{17}$$

where the size function is the usual normalized lognormal form [see, for instance, *Yue*, 1986] with parameters r_0 and $\ln(s)$. The altitude dependence of the aerosol number density is a Gaussian function peaking at $z = z_0$ to represent an aerosol layer of thickness Δ. Hereinafter we will refer to the "standard" volcanic case for the following values of the parameters extracted from the literature [*Russell et al.*, 1996]:

$$n_0 = 10 \text{ cm}^{-3},\; z_0 = 20 \text{ km},\; \Delta = 5 \text{ km},\; \ln(s)$$

$$= 0.452,\; r_0 = 0.3 \; \mu\text{m} \tag{18}$$

For $Q(\lambda, r)$ we have used the anomalous diffraction approximation described by *van de Hulst* [1957]:

$$Q(\lambda, r) = \pi r^2 \left(2 - \frac{2}{\gamma r} \sin(2\gamma r) + \frac{1}{(\gamma r)^2} (1 - \cos(2\gamma r)) \right) \tag{19}$$

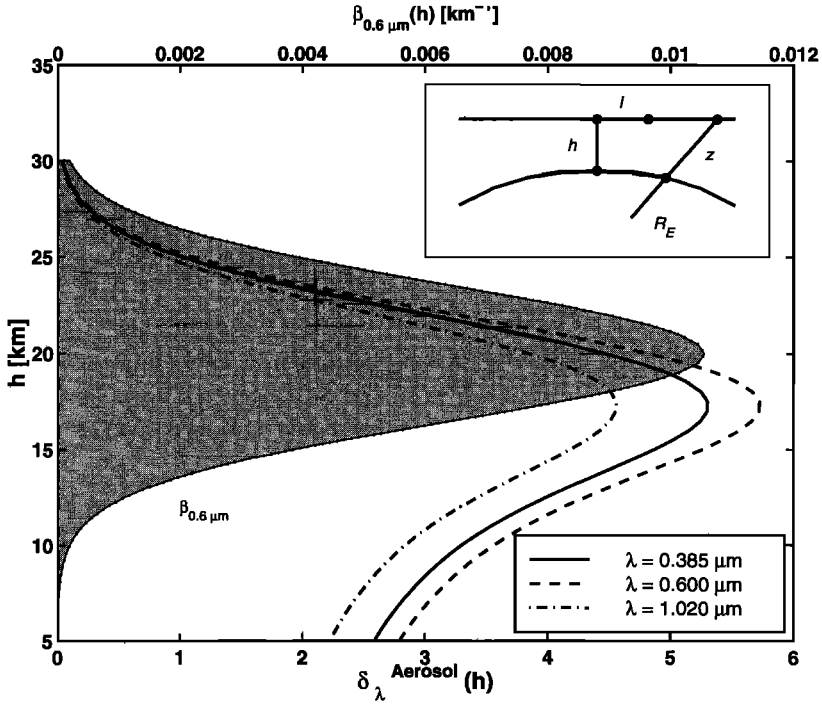

Figure 1. Inset shows the occultation geometry. The upper curve shows the aerosol extinction coefficient (shaded area, upper x axis) at $\lambda = 0.6$ μm for the "standard" volcanic case (equation (18)) as a function of altitude h. The lower curves show the slant path aerosol optical thickness (lower x axis) as a function of the tangent height for three channels of SAGE II. Notice that the maximum of the optical thickness is shifted downward due to the contributions from higher altitudes.

$$\gamma = \frac{2\pi(n_r - 1)}{\lambda} \tag{20}$$

where n_r (equal to 1.43) is the refraction index. It has been checked that the values produced by (19) do not differ from the results of exact Mie computations by more than 20% and contain the essential oscillatory structures.

The aerosol optical thicknesses $\delta_\lambda^{aerosol}$ have been numerically integrated using (1) and (9) (where β_λ was replaced by $\beta_\lambda^{aerosol}$) and assuming a rectilinear trajectory for the ray path. Indeed, the wavelength dependence of atmospheric refractive effects is weak and is not expected to affect our conclusions for the considered altitudes. Furthermore, the Earth's surface has been approximated by a paraboloid at the grazing point so that the relation between altitude z and path length element l is given by

$$z = h + \frac{l^2}{2R_E} \tag{21}$$

where R_E stands for the Earth's radius (see Figure 1).

4. The Interpolation Problem

The variation of the aerosol optical thickness versus the tangent height h is presented in Figure 1 for the standard case. Owing to the occultation geometry, the maximum value of the slant path optical thickness is at a lower altitude ($h \simeq 18$ km) than the maximum in the aerosol extinction profile. It is also interesting to keep h fixed (Figure 2) ($h = 20$, 30 km) and to plot the evolution of $\delta^{aerosol}$ versus λ. All curves are very smooth because the integration over the particle radii tends to cancel the oscillatory structures associated with (19). On the other hand, the curves exhibit broad maxima in the range $\lambda \simeq 0.5 - 0.7$ μm, which may be understood as in relation with the mean particle radius $r_m = 0.3$ μm shifted toward larger values due to the r^2 leading factor in (19).

It is well known that the factor Γ in (12) acts as a regularization parameter for stabilizing the solution of an ill-conditioned inversion problem. However, it is interesting to analyze the accuracy of (13) in the case of an ideal noiseless experiment. This could assert a lower bound of the interpolation error because noise is expected to only degrade the results.

In case of $\Gamma = 0$, equation (12) reduces to the Moore-Penrose pseudo-inverse of matrix Q [see *Nash*, 1990], which can be considered as a zero-order regularization method [*Press et al.*, 1992], i.e., it produces a minimal norm solution of (11).

In Figure 3, we have reported the relative error of the aerosol optical thickness (see equation (26) for definition) obtained by using (12) (with $\Gamma = 0$, $R = (0.5, 1.0$ μm), and $dr = 0.01$ μm) when r_0 and $\ln(s)$ are varied around the standard case. In Figure 3 we also report the relative error computed by using the SAGE II operational interpolation coefficients α_i (see equation (14)). The later computation confirms the results obtained by *Steele and Turco* [1997] in an independent approach: The SAGE II interpolation algorithm tends to underestimate the aerosol optical thickness at 0.6 μm for large r_0 values (usually associated with volcanic aerosol) and to overestimate it for background aerosol. By inspecting (3), it is obvious to see that this interpolation error would imply an overestimation and an underestimation, respectively, of the O_3 optical thickness. If the measurements started in a period of high volcanic aerosol mass loading (in 1984, after El Chichon eruption) and continued until a low aerosol level (in 1991,

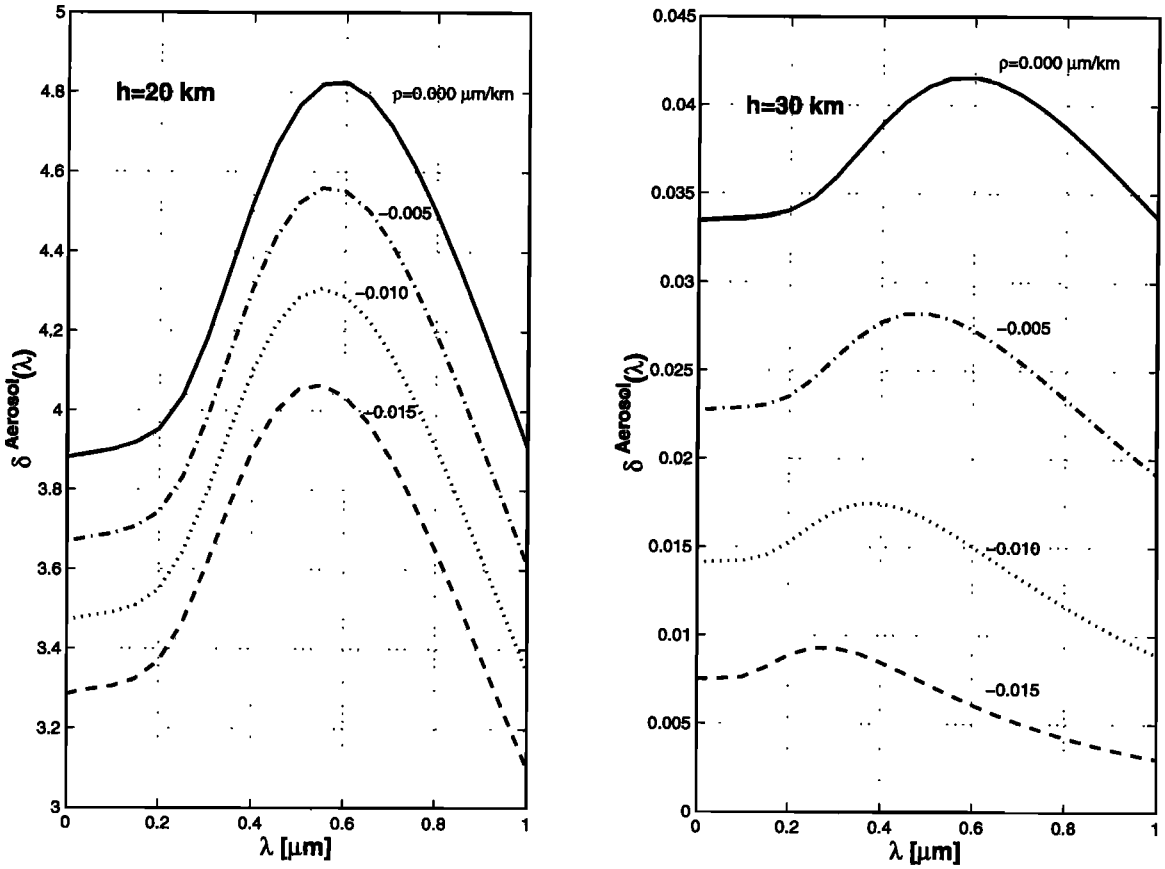

Figure 2. The slant path aerosol optical thickness at (left) h = 20 km and (right) h = 30 km versus wavelength. Different gradients ρ of the mean particle radius are considered (see equation (35)). The standard case corresponds to $\rho = 0$.

before Pinatubo), this may give rise to the exaggerated negative ozone trend observed by *Cunnold et al.* [1996].

More amazing is the dependence of the results obtained by using (12) and (13) on the upper bound R chosen for the particle size distribution, even at values for which the total optical thickness has converged! This is illustrated in Figure 4, where aerosol retrieval relative errors as large as 15% have been found. Such large errors are, of course, unacceptable because the optimal R, if any, to be used is closely related to the unknown size distribution (the R value used by *Chu et al.* [1989] is unclear). The same dependence of the interpolating coefficients on R has been mentioned by *Steele and Turco* [1997] and casts serious doubts on the possibility of a 1% accuracy for both aerosol and ozone retrievals.

We propose a simple explanation for this systematic aerosol prediction error. The main point is that (10)–(14) are not wrong but rather inadequate to solve the problem. Indeed, as already mentioned, system (10) is largely underdetermined, allowing an infinite number of solution vectors $\vec{N}$. This is nothing more than an inversion problem for which there is little hope of obtaining a large number of significant parameters for the unknown particle size distribution. The Twomey solution is a regularization method [see, for example, *Press et al.*, 1992], trying to select one solution among the infinite set with respect to a constraint related to the experimental estimated noise (this constraint is reasonable but nevertheless arbitrary). In that sense, one can say that the solution vector $\vec{N}$ (equation (12)) is "optimal" to solve the inverse problem.

A correct explanation of the somewhat wavy behavior of the relative error observed in Figure 4 has nothing to do with instability as it is often invoked. Indeed, instability is closely related with redundancy between different measurements at different wavelengths, which, in turn, induces very small eigenvalues and associated sensitivity in the inverse or the pseudo-inverse of the Q matrix.

On the other hand, it is clear that the information content about $f(r)$ that can be retrieved from four independent measurements at 0.385, 0.453, 0.525, and 1.02 μm is limited and cannot exceed four independent pieces of information. This "incompleteness" of the measurement (also referred to as the null-space error) has often been disregarded as an important error source. However, there does not exist a regularization method capable of recovering missing information from the data set. More quantitatively and following *Twomey* [1985], one may decompose the unknown slant path integrated size distribution $N(r)$ as

$$N(r) = N^{\parallel}(r) + N^{\perp}(r) \tag{22}$$

with

$$N^{\parallel}(r) = \{\xi_1\phi_1(r) + \xi_2\phi_2(r) + \xi_3\phi_3(r) + \xi_4\phi_4(r)\} \tag{23}$$

or

$$N^{\parallel}(r) = \vec{\xi}^T \cdot \vec{\phi}(r) \tag{24}$$

where $N^{\parallel}(r)$ and $N^{\perp}(r)$ refer to the subspaces parallel and orthogonal, respectively, to the four measurement kernels. The

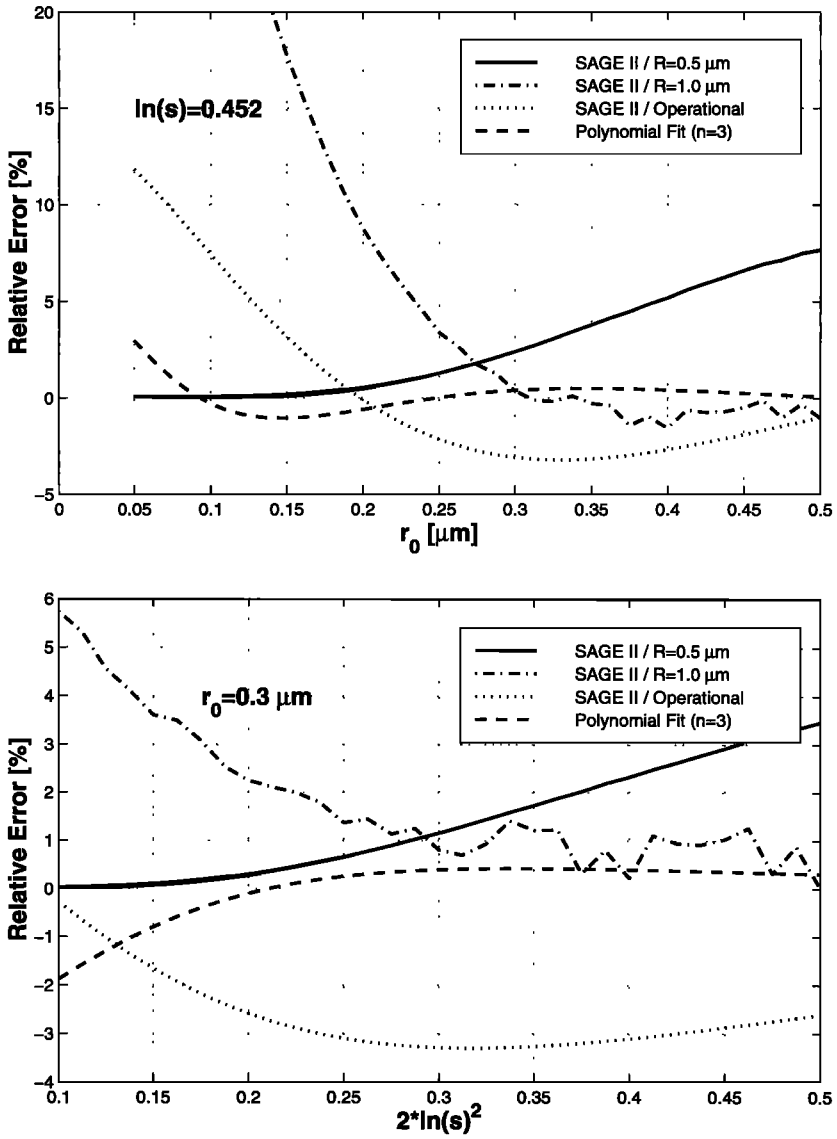

Figure 3. (top) Relative error on the prediction of the slant path aerosol optical thickness at $\lambda = 0.6$ μm for different interpolation methods. The variance of the particle size distribution is kept fixed at its standard value, and the mean radius is varied. (bottom) Same as above, but r_0 is kept fixed and the variance is varied.

$\phi_j(r)$ are the orthonormalized eigenvectors of the the symmetric covariance matrix C defined by

$$C_{ij} = \int_0^R Q(\lambda_i, r)Q(\lambda_j, r)\, dr \tag{25}$$

and $\vec{\xi}$ is the array of expansion coefficients in the considered basis.

The relative error when interpolating the slant path aerosol optical thickness at $\lambda = 0.6$ μm is

$$E = \frac{x_3 - x_3^{\text{exact}}}{x_3^{\text{exact}}} \tag{26}$$

where

$$x_3 = \vec{\alpha}^T \cdot (\vec{x}^{[0,R]} + \vec{x}^{[R,\infty]}) \tag{27}$$

with

$$\vec{x}_i^{[0,R]} = \int_0^R Q(\lambda_i, r)N(r)\, dr \ \{i = 1, 4, 5, 7\} \tag{28}$$

$$\vec{x}_i^{[R,\infty]} = \int_R^\infty Q(\lambda_i, r)N(r)\, dr \ \{i = 1, 4, 5, 7\} \tag{29}$$

For an accurate interpolation scheme we have

$$\vec{\alpha}^T \cdot \vec{x}^{[0,R]} \simeq \int_0^R Q(0.6, r)N^{\parallel}(r)\, dr \tag{30}$$

This allows us to express the relative error E as the sum of two terms:

$$E = E_{\text{NS}} + E_T \tag{31}$$

where E_{NS} is the null-space relative error defined by

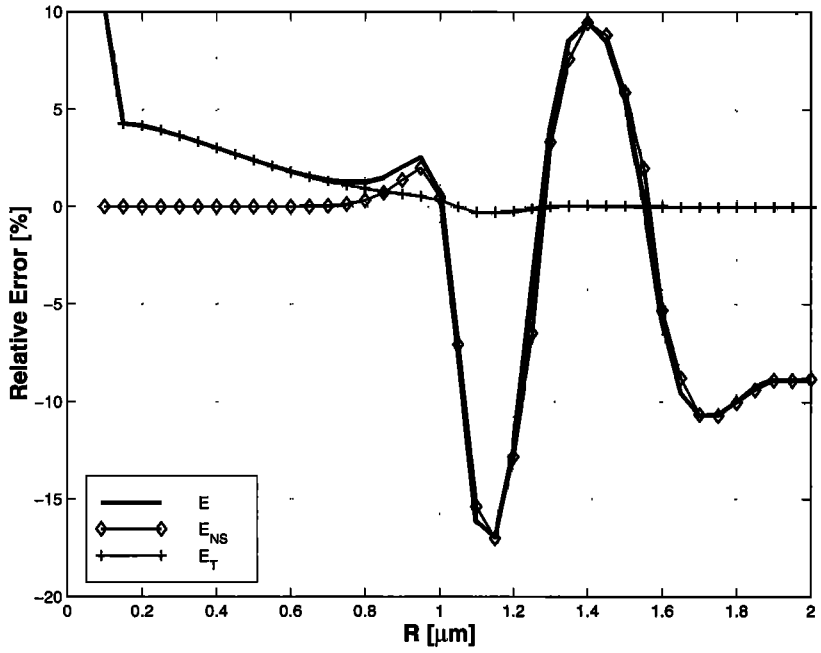

Figure 4. Behavior of the relative error on the aerosol optical thickness at $\lambda = 0.6$ μm as R, the upper bound of the considered particle radius, is varied (see equation (31)).

$$E_{NS} = \frac{-\int_0^R Q(0.6, r)N^{+}(r)\,dr}{x_3^{exact}} \tag{32}$$

and E_T is the truncation relative error:

$$E_T = \frac{\left(-\int_R^{\infty} Q(0.6, r)N(r)\,dr + \vec{\alpha}^T \cdot \vec{x}^{[R,\infty]}\right)}{x_3^{exact}} \tag{33}$$

The E_{NS} contribution gets more important for large R values (see Figure 4) because the kernel $Q(\lambda, r)$ is not a square-integrable function, and the four-channel sampling becomes less and less representative as R increases.

On the other hand, reducing the value of R leads to the truncation of the size distribution, corrected, however, by the term $\vec{\alpha}^T \cdot \vec{x}^{[R,\infty]}$. This correction is imperfect because the array of interpolating coefficients $\vec{\alpha}$ has been determined over the range $[0, R]$ in place of the full range $[0, \infty]$. The results obtained above indicate that the prediction of the aerosol contribution at 0.6 μm should not be formulated as an inversion problem requiring the delicate derivation of the particle size distribution because both null-space and truncation errors depend on the unknown distribution itself.

Instead, it would more profitable to derive the value of x_3 from a smooth interpolating function. Any candidate capable of reproducing the wavelength behavior of the aerosol optical thickness $\delta_\lambda^{aerosol}$ by using a least squares procedure could be chosen, but a simple third-order polynomial is an evident possibility:

$$\delta_\lambda^{aerosol} \simeq c_0 + c_1\lambda + c_2\lambda^2 + c_3\lambda^3 \tag{34}$$

This choice is justified because almost any nonpathological size distribution leads after integration to a smooth wavelength dependence of the optical thickness. Therefore the difficult problem of determining the optimal regularization for an underlying unknown distribution is replaced by a simple smoothness constraint on its integral which is easily verified by a polynomial. Once again, we underline that the choice of a polynomial in λ is arbitrary and that many other forms could be used, for instance, the one depending on $\ln(\lambda)$ in the Laboratoire d'Optique Atmosphérique (LOA) algorithm [see *Chu et al.*, 1989]. The main point is that the determination of the optimal R value is now irrelevant.

It can be seen in Figure 3 that the relative error obtained by using (34) seems to be more satisfactory than the SAGE II solution. It is also worth noting that the simple polynomial fit procedure has been successfully used by *Amato et al.* [1996].

In order to analyze the noise sensitivity of the generic SAGE II and of the polynomial interpolation methods, we have performed a Monte Carlo simulation of the relative error on x_3 when Gaussian noise is added to the four measurement channels. In Figure 5 we present the results of this simulation when the relative amplitude (which may depend on signal saturation due to a large volcanic activity) of the noise is varied. A common relative amplitude has been taken, but in all simulations the noise component is randomly added to each channel independently. For the generic SAGE II algorithm we have chosen $R = 1.0$ μm with a diagonal matrix Γ (as described by *Chu et al.* [1989]), whose elements are the estimated absolute noise levels in the respective channels. The relative errors of both interpolation schemes are roughly the same for a noiseless realization of the standard case, but this is, of course, fortuitous, as can be seen in Figure 3.

When the noise amplitude is increased, we have reported in Figure 5 the mean error of the distribution of simulations and also the limits corresponding to a standard deviation of the statistical distribution of the results. At first sight, both schemes exhibit a comparable sensitivity to the noise amplitude, but it is somewhat higher for the polynomial interpolation. On the other hand, the SAGE II method seems to pro-

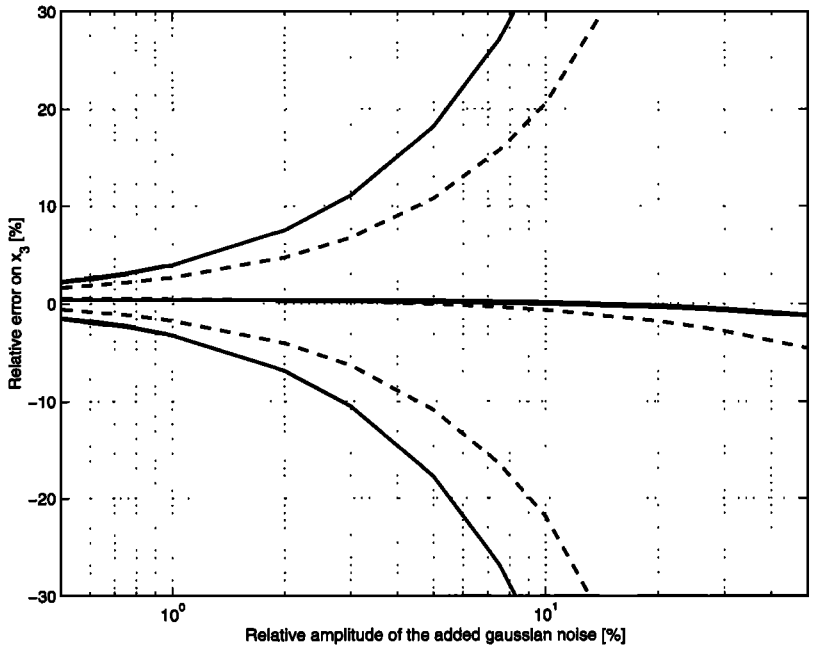

Figure 5. Evolution of the relative error on the aerosol optical thickness at $\lambda = 0.6$ μm as the relative amplitude of the added Gaussian noise increases. Dashed curves denote generic SAGE II interpolation method (mean value and mean value plus or minus the standard deviation), and solid curves denote the same for the polynomial interpolation method.

duce a mean relative error slightly more biased when the noise amplitude gets larger. We conclude that both interpolation schemes behave quite similarly in the presence of noise, which is not very surprising because the Γ term in (12) does not prevent the SAGE II interpolation from being sensitive to measurement errors. Instead, the role of Γ is to cancel the effects of the smallest (and then negligible) eigenvalues of QQ^T which are responsible for the instability in the inversion of the particle size distribution (see *Twomey* [1985] for a detailed discussion).

5. The Vertical-Spectral Coupling

The interpolation accuracy itself is not so bad for the aerosol optical thickness retrieval as for the ozone retrieval where accuracies better than 1% are hoped to monitor long-term trends. On the other hand, we think there is another reason in the SAGE II spectral inversion algorithm for inducing an inaccurate x_3 interpolation.

By inspecting (17), it is clear to see that the aerosol size distribution function has been factorized in an altitude concentration function times a relative size distribution function characterized by the parameters r_0 and $\ln(s)$. However, there exist experimental and theoretical arguments for r_0 and $\ln(s)$ being altitude-related parameters. For instance, concentrating on r_0 only, we may approximate the unknown altitude dependence by a simple linear variation:

$$r_0(z) \simeq r_{z_0} + \rho(z - z_0) \tag{35}$$

It is probable that ρ has mostly a negative value because smaller particles are expected to be dominant at higher altitudes, as suggested by the sedimentation process. In Figure 2 we have also reported δ (λ) for different values of ρ. When ρ is different from 0, the ratio $\delta(0.6)/\delta$ (0.525) may be greater or less than 1, depending on the altitude, and the relative shapes of the curves are somewhat different.

Besides the evolution of the wavelength dependence of $\delta_\lambda^{\text{aerosol}}$ as the tangent height increases, the change of the mean radius corresponds to a contraction of the particle size distribution producing a variation of the relative error on x_3 (see Figure 3). In the generic SAGE II interpolation formula (equation (14)), the interpolating coefficients are fixed quantities (for assumed scattering model, aerosol composition, and refraction index). It is clear, however, that the interpolation error depends on the form of the interpolated function, and the optimal R value should be altitude dependent if the size distribution is also altitude dependent (see Figure 6). This has been recognized very recently [*Smalley*, 1997] as a critical point for developing version 5.95 of the SAGE II algorithm, and it is accepted that no single set of linear coefficients can fit the data for the whole family of aerosol distributions.

Starting from an assumed analytical shape of the particle size distribution, it is possible to extract the best mean radius that reproduces the observed spectral dependence of the aerosol extinction coefficient. Values of this mean radius have been published [*Brogniez et al.*, 1992; *Thomason*, 1991] that clearly show an important altitude dependence.

A possible remedy could consist of using the altitude dependence of the retrieved mean radius to optimize the R value as a function of tangent height and to produce an altitude-dependent set of coefficients. The spectral-vertical inversion should then be iterated once more, and convergence of the results could be checked.

A second example of spectral-vertical coupling can be found by considering a possible altitude dependence of the refraction index which may be related to composition change of the aerosol. In a first approximation we suppose that this dependence is linear, as

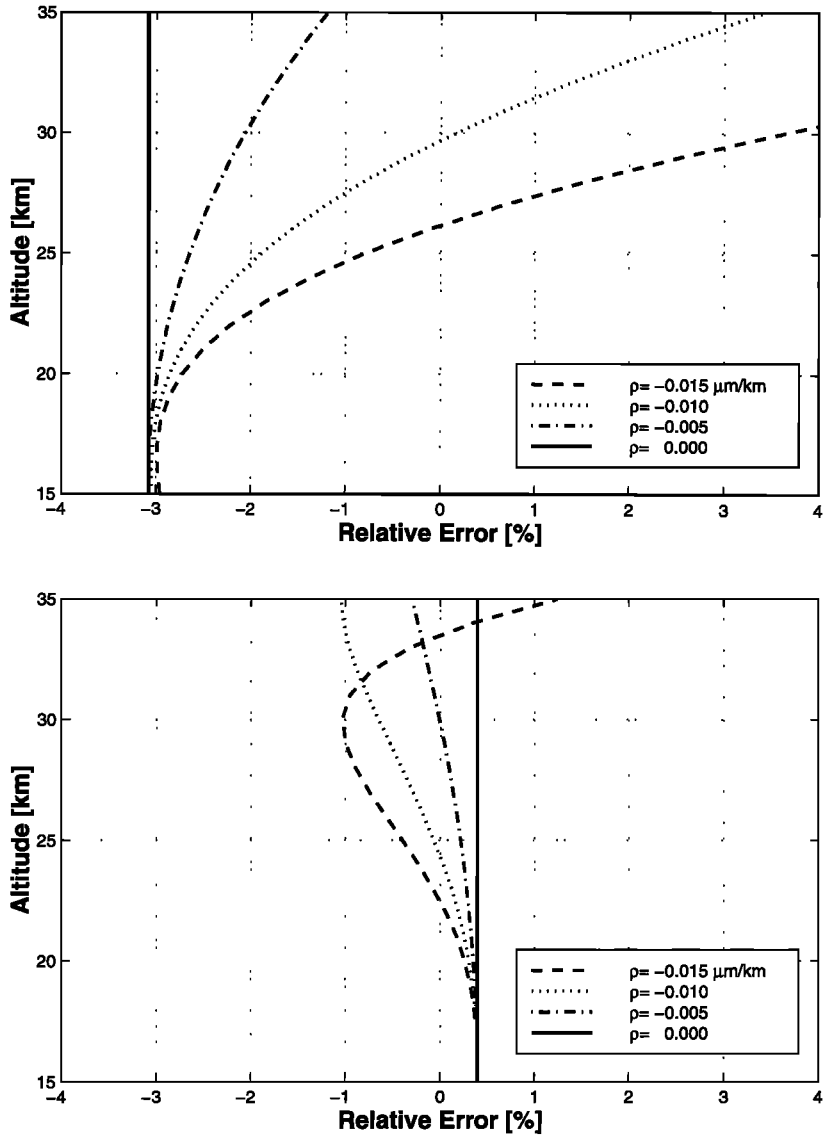

Figure 6. (top) Evolution of the relative error on the aerosol optical thickness at $\lambda = 0.6$ μm versus the altitude for different gradients of the mean radius, by using the SAGE II operational interpolation scheme. (bottom) Same as above but for the polynomial interpolation.

$$n_r(z) \simeq n_r(z_0) + \kappa(z - z_0) \tag{36}$$

where κ is the gradient of the refraction index. In Figure 7 we report the evolution of the relative error on x_3 for both SAGE II operational and polynomial interpolation schemes. The former seems to be more sensitive to the value of κ. This is not astonishing because an altitude-dependent refraction index does not allow us to factorize the Mie cross section $Q(\lambda, r)$ out of the optical path integration leading to (10).

6. Conclusions

We have analyzed the SAGE II ozone retrieval algorithm and the origin of a bias due to aerosol contamination. Independent of strong variations of the particle size distribution in the case of high volcanic mass loading, we have pointed out two possible causes of inaccuracy in the generic SAGE II algorithm for predicting the aerosol optical thickness at 0.6 μm. The interpolation problem can be probably easily solved by avoiding formulating it as an inverse problem as mentioned above because the optimization of the inversion method depends on the unknown size distribution.

The spectral-vertical decoupling seems a much more complicated task because there is no means of knowing whether a variation in the slant path aerosol optical thickness is caused by the altitude variation of the aerosol number density or by the variation of its spectral properties. Furthermore, different quantities may be implied as, for instance, the mean radius r_0, the standard deviation $\ln(s)$, or the refractive index n_r. This could require the selection of a different order for the inversions, i.e., vertical first, spectral second [see *Chu et al.*, 1989], for which the amount of work has to be compared with respect to the gained accuracy. Indeed, in this approach, which has been implemented by the LOA group in order to validate the SAGE II generic algorithm, the total extinction coefficient is computed first for each stratospheric layer before the species separation. On the other hand, empirical correction strategies

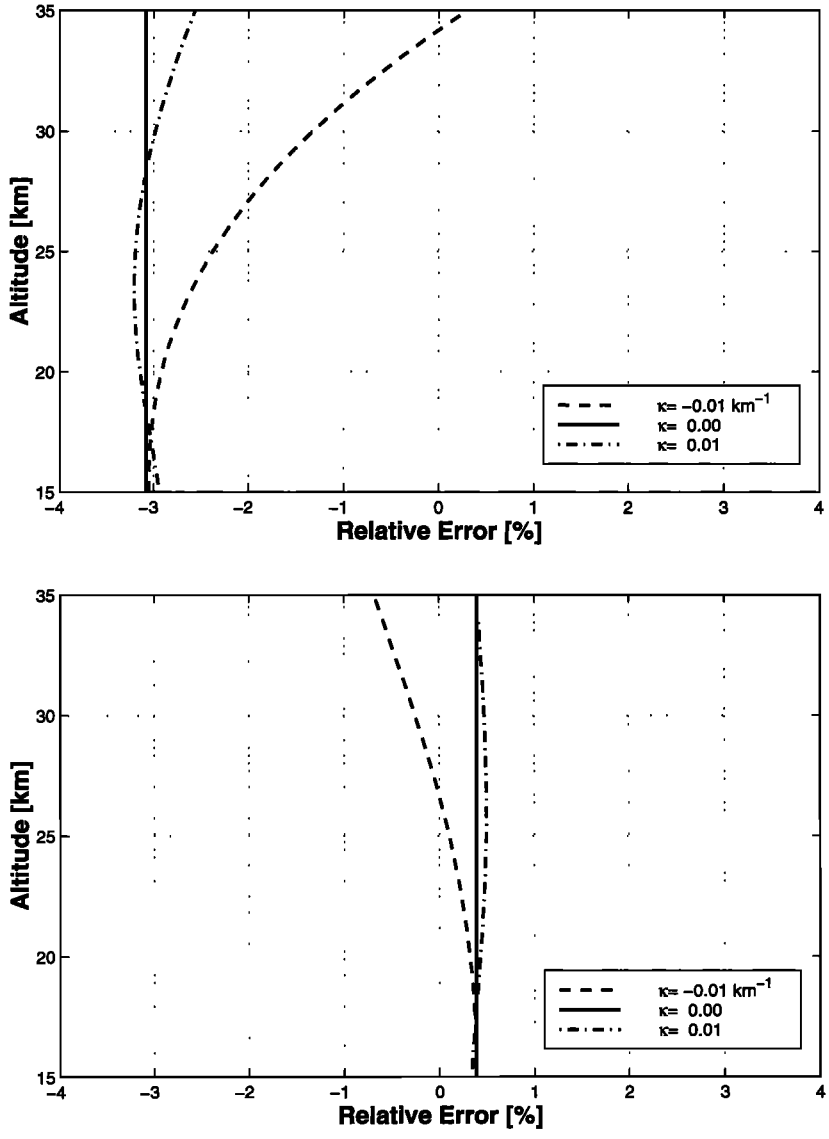

Figure 7. (top) Evolution of the relative error on the aerosol optical thickness at $\lambda = 0.6$ μm versus the altitude for different gradients of the refraction index, by using the SAGE II operational interpolation scheme. (bottom) Same as above but for the polynomial interpolation.

have been proposed by *Cunnold et al.* [1996], but they are probably not optimal for accurate and long-term monitoring of the ozone trends.

Acknowledgments. The author expresses his gratitude to G. Kockarts, head of the Department of Theoretical Aeronomy at the Belgian Institute for Space Aeronomy, for careful reading of the manuscript and comments and suggestions. He is also grateful to H. Steele and R. Turco of the Department of Atmospheric Sciences at the University of California for having communicated to him a preprint version of their paper. This work was partly supported by the "Fonds National de la Recherche Scientifique" of the Belgian Government under contract 1.5.207.95F.

References

Amato, U., D. Di Bello, F. Esposito, C. Serio, G. Pavese, and F. Romano, Intercomparing the Twomey method with a multimodal lognormal approach to retrieve the aerosol size distribution, *J. Geophys. Res.*, *101*, 19,267–19,275, 1996.

Brogniez, C., R. Santer, B. S. Diallo, M. Herman, J. Lenoble, and H. Jäger, Comparative observations of stratospheric aerosols by ground-based lidar, balloon-borne polarimeter, and satellite solar occultation, *J. Geophys. Res.*, *97*, 20,805–20,823, 1992.

Chu, W. P., M. P. McCormick, J. Lenoble, C. Brogniez, and P. Pruvost, SAGE II inversion algorithm, *J. Geophys. Res.*, *94*, 8339–8351, 1989.

Cunnold, D. M., and R. E. Veiga, Preliminary assessment of possible aerosol contamination effects on SAGE ozone trends in the lower stratosphere, *Adv. Space Res.*, *11*(3), 5–8, 1991.

Cunnold, D. M., H. Wang, W. P. Chu, and L. Froidevaux, Comparisons between Stratospheric Aerosol and Gas Experiment II and Microwave Limb Sounder ozone measurements and aliasing of SAGE II ozone trends in the lower stratosphere, *J. Geophys. Res.*, *101*, 10,061–10,075, 1996.

Hood, L. L., R. D. McPeters, J. P. McCormack, L. E. Flynn, S. M. Hollandsworth, and J. F. Gleason, Altitude dependence of stratospheric ozone trends based on NIMBUS 7 SBUV data, *Geophys. Res. Lett.*, *20*, 2667–2670, 1993.

Mauldin, L. E. III, N. H. Zaun, M. P. McCormick, J. H. Guy, and W. R. Vaughn, Stratospheric Aerosol and Gas Experiment II instrument: A functional description, *Opt. Eng.*, *24*, 307–312, 1985.

Nash, J. C., *Compact Numerical Methods for Computers*, Adam Hilger, New York, 1990.

Press, W. H., S. A. Teukolsky, W. T. Vetterling, and B. P. Flannery, *Numerical Recipes in FORTRAN*, 2nd ed., Cambridge Univ. Press, New York, 1992.

Russell, P. B., et al., Global to microscale evolution of the Pinatubo volcanic aerosol, derived from diverse measurements and analyses, *J. Geophys. Res.*, *101*, 18,745–18,763, 1996.

Smalley, S., Minutes of the SAGE II meeting, *The Earth Observer*, *9/1*, NASA Goddard Space Flight Cent., Greenbelt, Md., 1997.

Steele, H. M., and R. P. Turco, Separation of aerosol and gas components in the Halogen Occultation Experiment and the Stratospheric Aerosol and Gas Experiment (SAGE II) extinction measurements: Implications for SAGE II ozone concentrations and trends, *J. Geophys. Res.*, *102*, 19,665–19,681, 1997.

Thomason, L. W., A diagnostic stratospheric aerosol size distribution inferred from SAGE II measurements, *J. Geophys. Res.*, *96*, 22,501–22,508, 1991.

Twomey, S., *Introduction to the Mathematics of Inversion in Remote Sensing and Indirect Measurements*, Elsevier Sci., New York, 1985.

van de Hulst, H. C., *Light Scattering by Small Particles*, Dover, Mineola, N. Y., 1957.

Wang, H. J., D. M. Cunnold, and X. Bao, A critical analysis of Stratospheric Aerosol and Gas Experiment ozone trends, *J. Geophys. Res.*, *101*, 12,495–12,514, 1996.

Yue, G. K., Wavelength dependence of aerosol extinction coefficient for stratospheric aerosols, *J. Clim. Appl. Meteorol.*, *25*, 1775–1779, 1986.

D. Fussen, Belgian Institute for Space Aeronomy (IASB-BIRA), 3, avenue Circulaire, B-1180 Bruxelles, Belgium. (e-mail: Didier.Fussen@oma.be)

(Received May 12, 1997; revised December 22, 1997; accepted December 22, 1997.)